

**Electrolytic conductivity-related radiofrequency heating of aqueous
suspensions of nanoparticles for biomedicine**

Supplementary Information

Konstantin Tamarov,^{a,b} Maxim Gongalsky,^{a,c} Liubov Osminkina,^{a,e}

Yuanhui Huang,^{c,d} Murad Omar,^{c,d} Valery Yakunin,^a

Vasilis Ntziachristos,^{c,d} Daniel Razansky,^{c,d} and Victor Timoshenko^{a,e}

^a*Faculty of Physics, M. V. Lomonosov Moscow State University, 119991 Moscow, Russia.*

^b*Department of Applied Physics, University of Eastern Finland, 70211 Kuopio, Finland*

^c*Institute of Biological and Medical Imaging, Helmholtz Zentrum München, 85764 Neuherberg,
Germany.*

^d*Chair of Biological Imaging, Technische Universität München, 80333 Munich, Germany*

^e*National Research Nuclear University "MEPhI", International Laboratory "Bionanophotonics",
115409 Moscow, Russia*

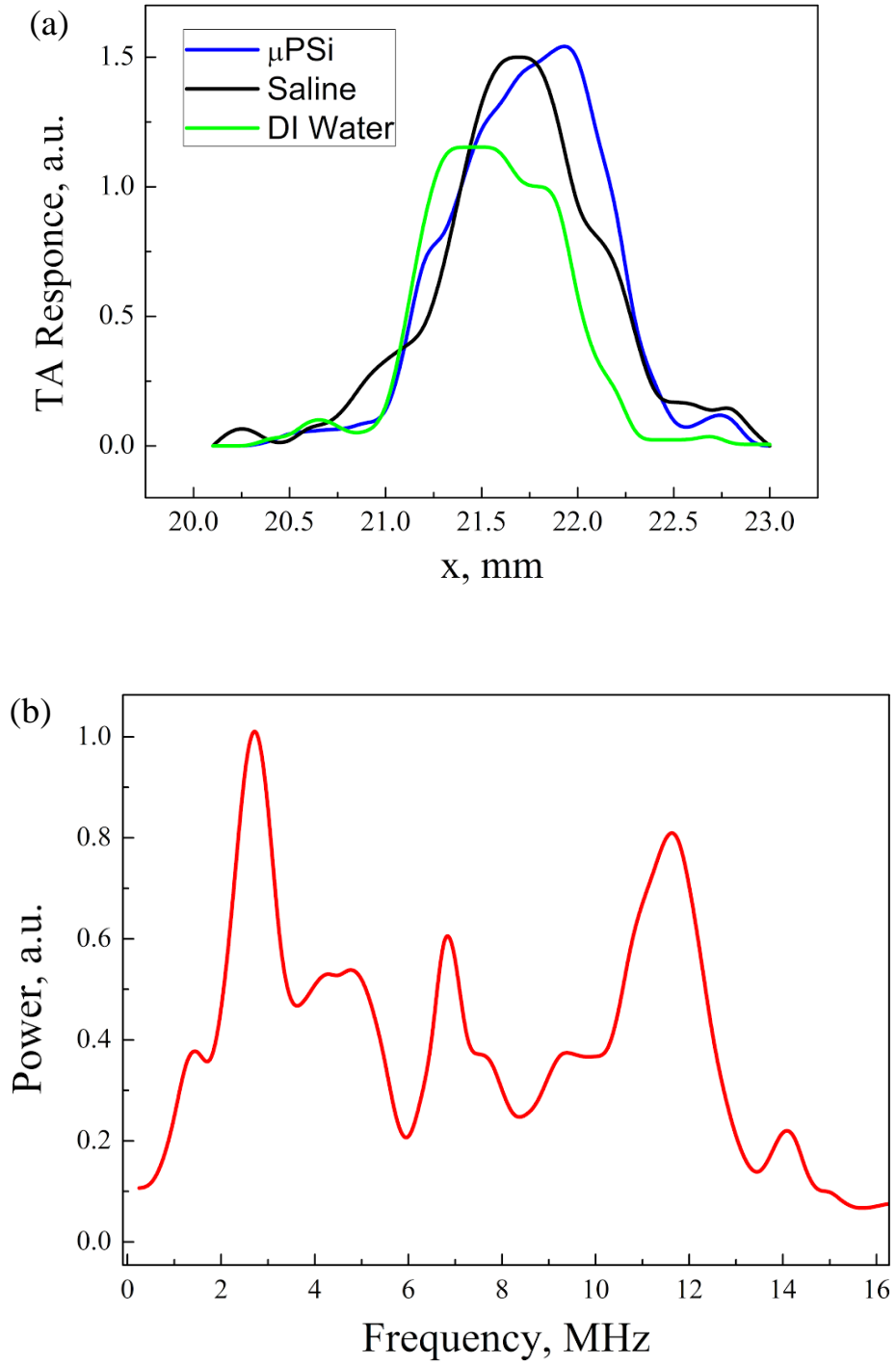


Figure S1. (a) Thermoacoustic response of distilled water (green line), saline (black line) and water suspension of μ PSi NPs; (b) spectrum of the thermoacoustic emission.

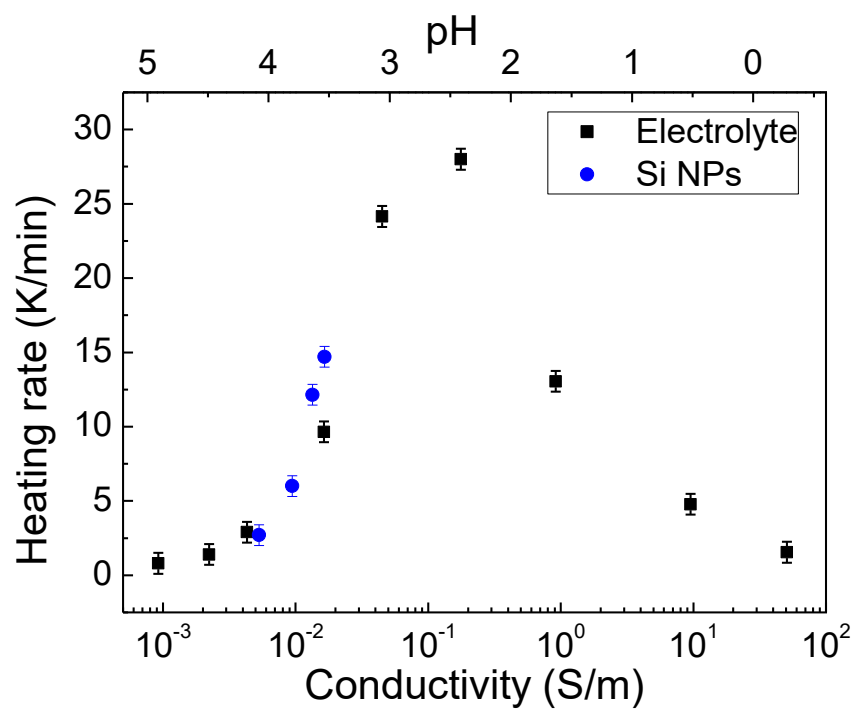
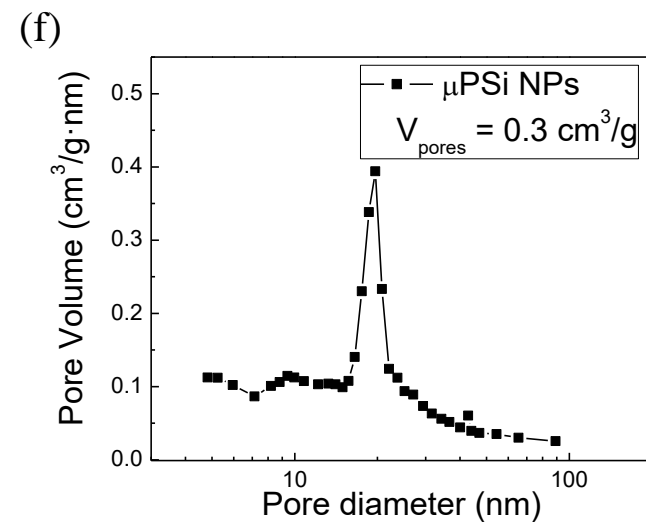
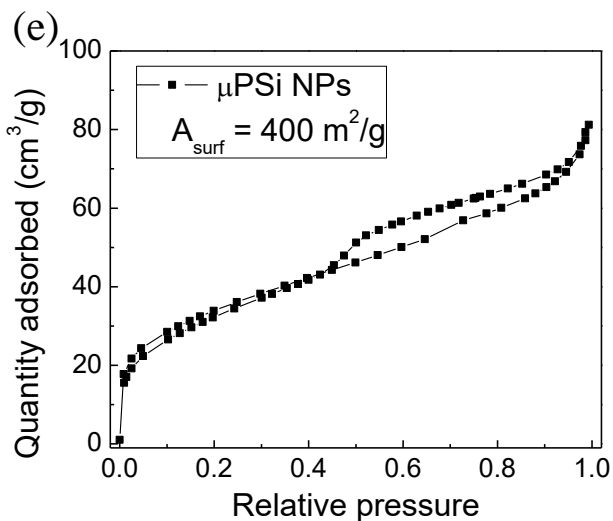
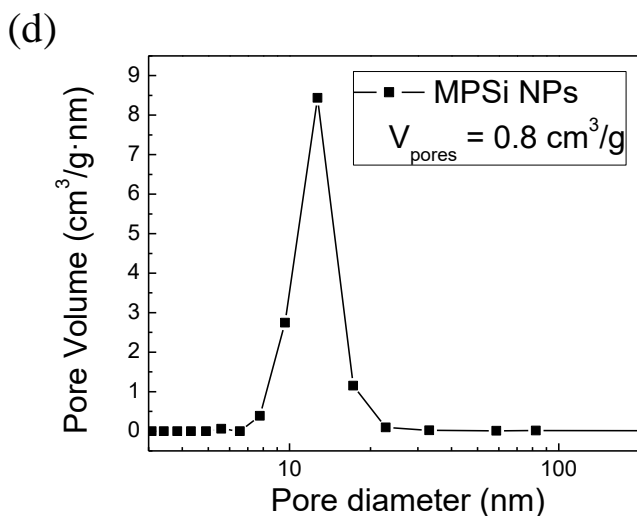
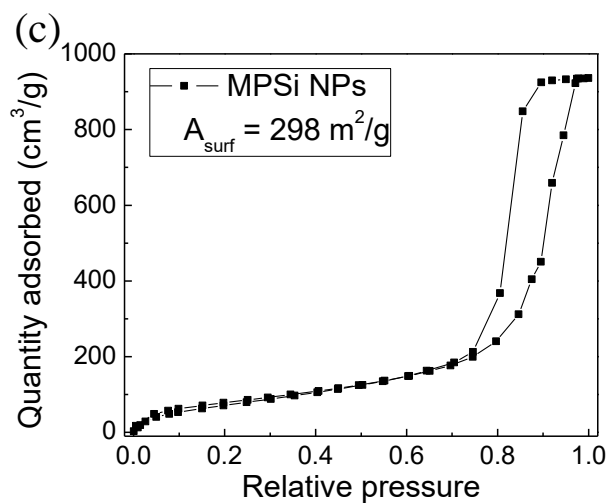
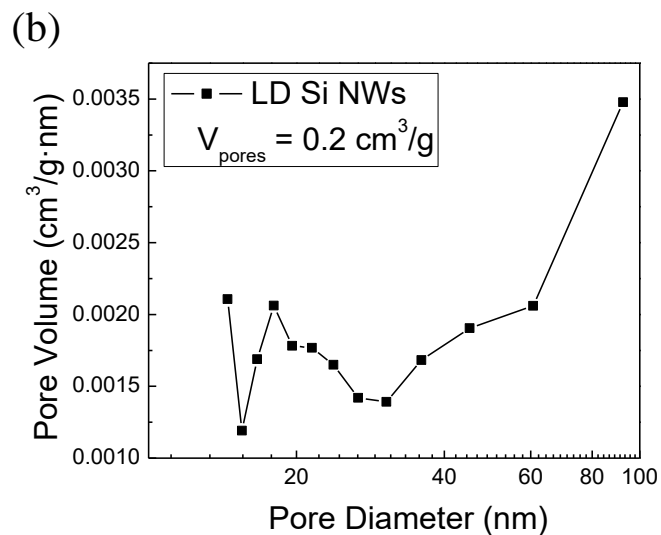
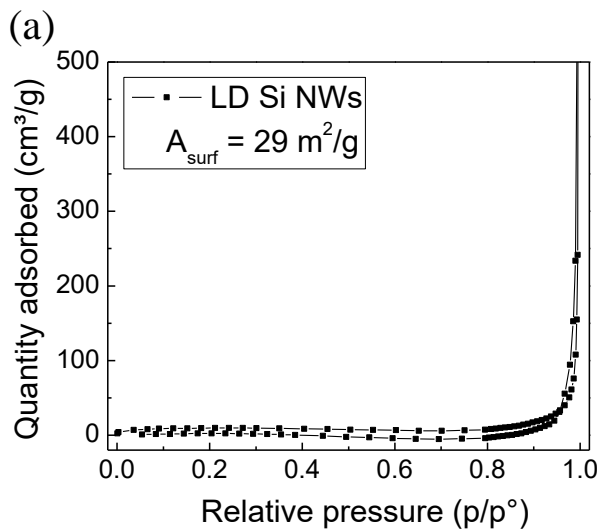


Figure S2. Heating rates of electrolyte solutions of different pH values (black squares) and aqueous suspensions of Si NPs (blue circles) under RF electromagnetic irradiation (27.12 MHz and 66 W).



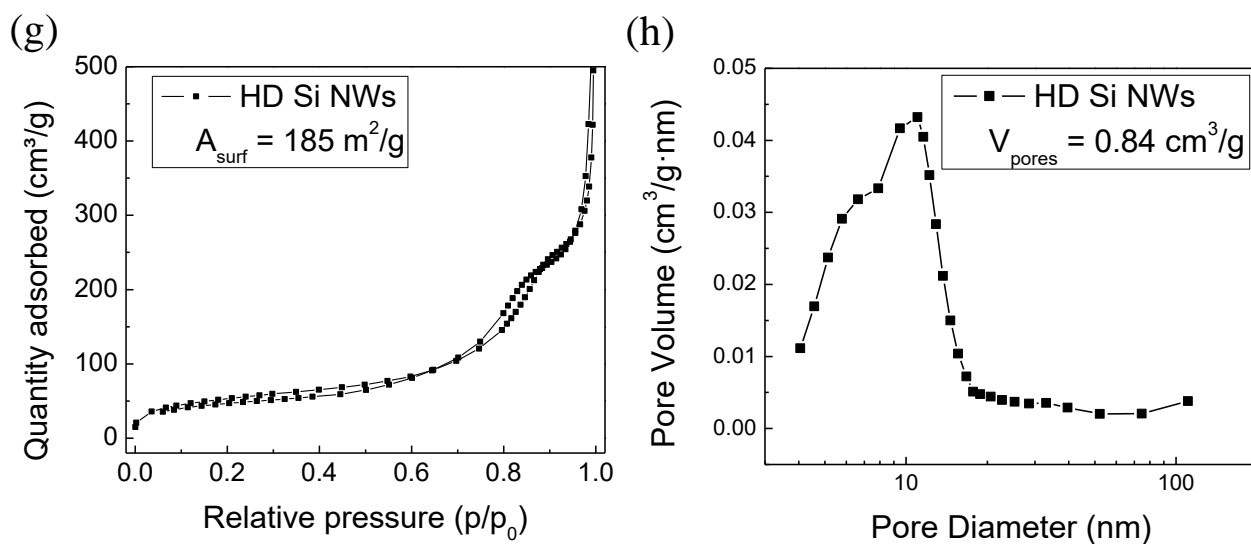


Figure S3. (a, c, e, g) N_2 adsorption-desorption isotherms and surface areas of LD Si NWs, MPSi NPs, μ PSi NPs and HD Si NWs respectively; (b, d, f, h) pore size distribution and pore volume of LD Si NWs, MPSi NPs, μ PSi NPs and HD Si NWs respectively.

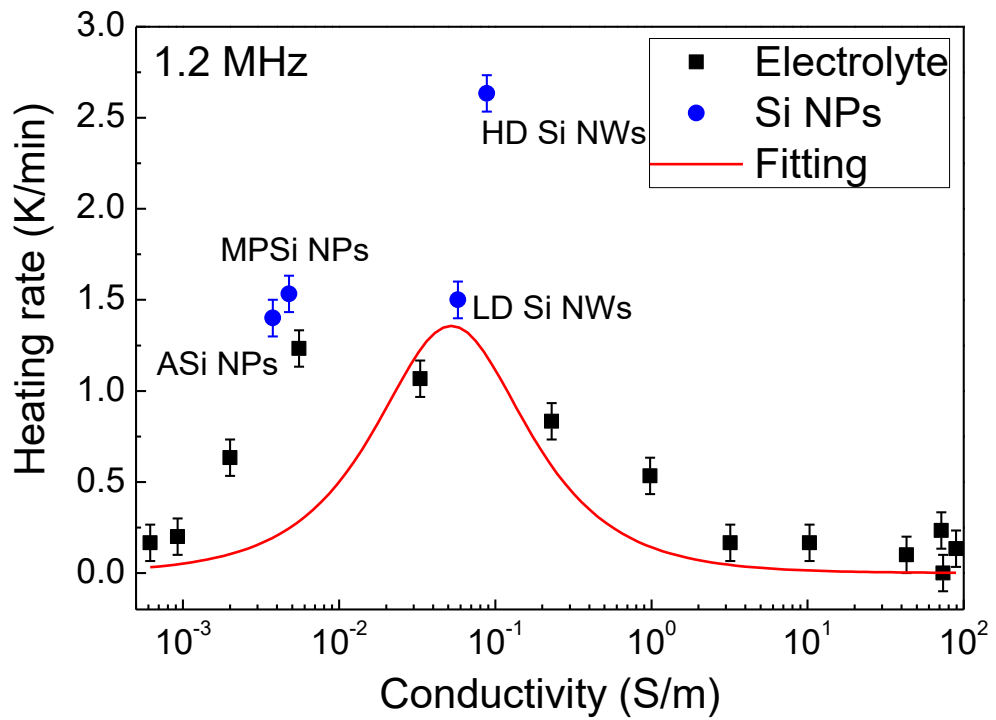


Figure S4. Heating rates of electrolyte solutions of different conductivities (black squares), aqueous suspension of Si NPs (blue circles) and fitting of the electrolyte heating rates according to the model (red line) under radiofrequency radiation of 1.2 MHz and 150 W. The fitting gives $\sigma_{\max} = (0.0053 \pm 0.0023)$ S/m which coincides within the error with theoretical value of 0.0051 S/m. Here, the heating maximum is not well pronounced and the heating rate is small, because at lower frequencies the equilibrium between E_{ext} and E_{int} is achieved faster than direction of external RF radiation changes.

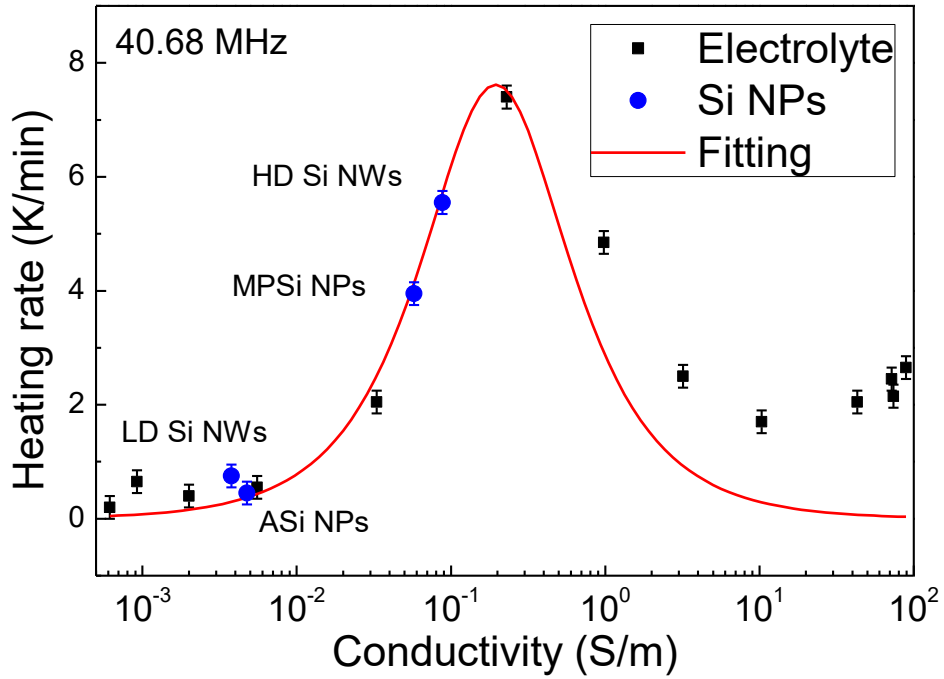


Figure S5. Heating rates of electrolyte solutions of different conductivities (black squares), aqueous suspension of Si NPs (blue circles) and fitting of the electrolyte heating rates according to the model (red line) under radiofrequency radiation of 40.68 MHz and 60 W. The fitting gives $\sigma_{\max} = (0.183 \pm 0.045)$ S/m which coincides within the error with theoretical value of 0.173 S/m. Here, the heating rate does not tend to zero for high values of conductivities. The discrepancy between can be explained by the absence of ion acceleration in the model. At higher frequency the external field changes its direction more often and neglected acceleration can start to play a bigger role and should be taken in into account in the ions motion process.

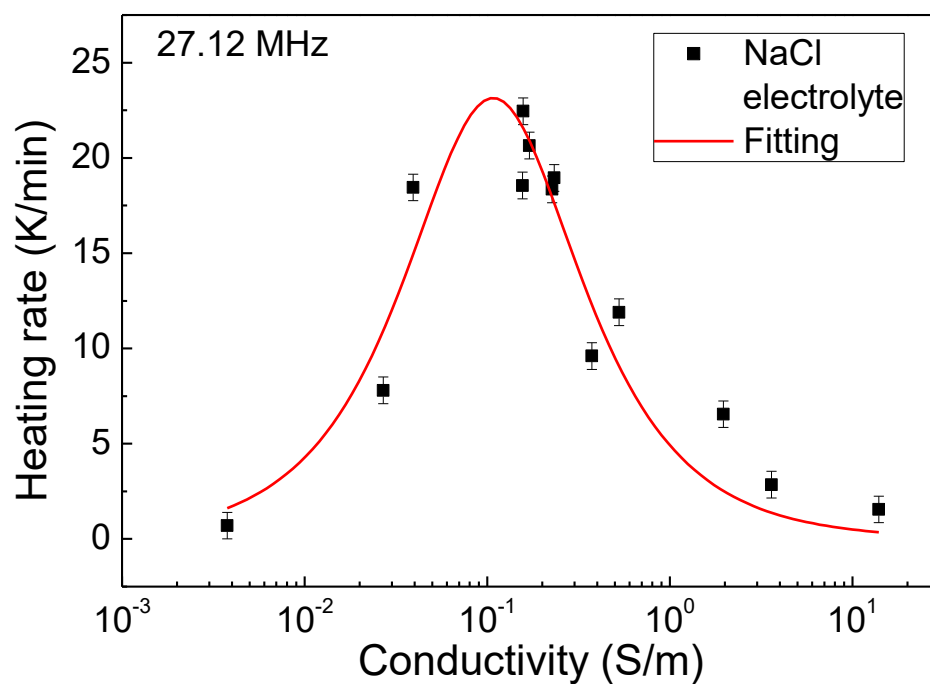


Figure S6. Heating rates of NaCl solutions of different conductivities (different concentration of NaCl) (black squares) and fitting of the electrolyte heating rates according to the model (red line) under RF irradiation (27.12 MHz, 66 W). The fitting gives $\sigma_{\max} = (0.11 \pm 0.01)$ S/m which coincides within the error with theoretical value of 0.115 S/m.

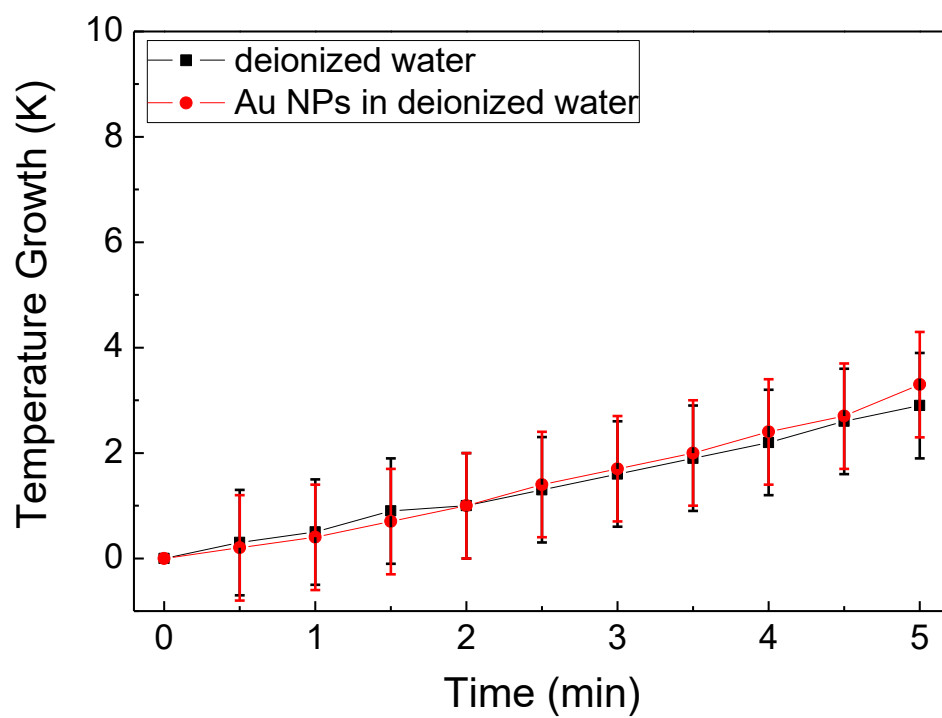


Figure S7. Temperature growth of deionized (black squares) water and 0.2 mg/ml Au NPs, dispersed in deionized water (red circles).

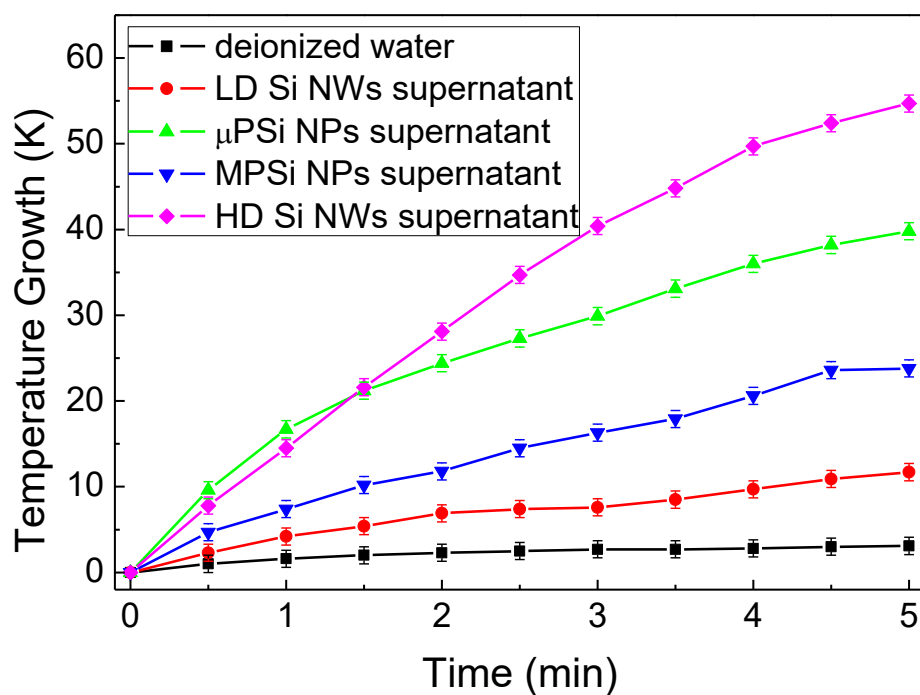


Figure S8. Temperature growth of filtered through $0.2 \mu\text{m}$ supernatant obtained from centrifugation of aqueous suspensions of various Si NPs from Figure 1 of the manuscript. The centrifugation was done at 20000 g for 20 min . The heating was performed at 27 MHz and 66 W . The heating rates are 14.5 K/min , 11.8 K/min , 5.9 K/min , 2.5 K/min for supernatants of HD Si NWs, μ PSi NPs, MPSi NPs and LD Si NWs, respectively. The heating rates are similar to the obtained for the suspensions.

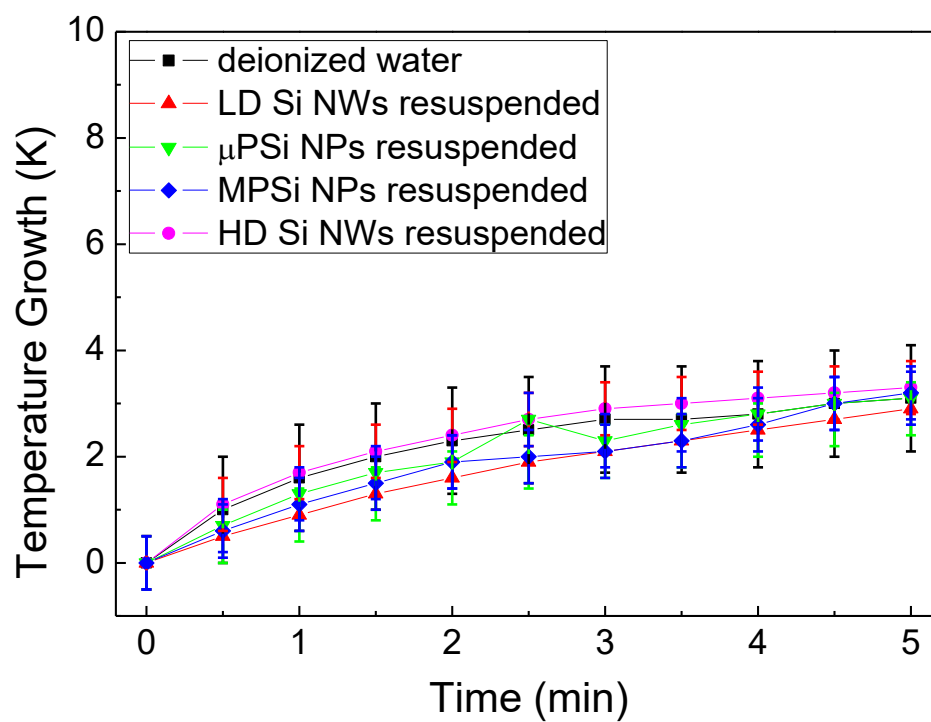


Figure S9. Temperature growth of aqueous suspensions of various Si NPs after resuspension in fresh deionized water.